doi:10.1006/jmbi.2001.4523 available online at http://www.idealibrary.com on IDEAL® J. Mol. Biol. (2001) 307, 967–976

JMB

COMMUNICATION

Phosphorylation Causes Subtle Changes in Solvent Accessibility at the Interdomain Interface of Methylesterase CheB

Carrie A. Hughes[1], Jeffrey G. Mandell[1], Ganesh S. Anand[2,3] Ann M. Stock[2,4,5] and Elizabeth A. Komives[1]*

[1]*Department of Chemistry and Biochemistry, University of California, San Diego, 9500 Gilman Dr, La Jolla CA 92093-0359, USA*

[2]*Center for Advanced Biotechnology and Medicine 679 Hoes Ln, Piscataway NJ 08854, USA*

[3]*Joint Graduate Program in Biochemistry, Rutgers University-University of Medicine and Dentistry of New Jersey, Piscataway NJ 08854, USA*

[4]*Department of Biochemistry University of Medicine and Dentistry of New Jersey, Robert Wood Johnson Medical School Piscataway, NJ 08854, USA*

[5]*Howard Hughes Medical Institute, 679 Hoes Ln. Piscataway, NJ 08854, USA*

**Corresponding author*

The crystal structure of the unphosphorylated state of methylesterase CheB shows that the regulatory domain blocks access of substrate to the active site of the catalytic domain. Phosphorylation of CheB at Asp56 results in a catalytically active transiently phosphorylated enzyme with a lifetime of approximately two seconds. Solvent accessibility changes in this transiently phosphorylated state were probed by MALDI-TOF-detected amide hydrogen/deuterium exchange. No changes in solvent accessibility were seen in the regulatory domain upon phosphorylation of Asp56, but two regions in the catalytic domain (199-203 and 310-317) became more solvent accessible. These two regions flank the active site and contain domain-domain contact residues. Comparison with results from the isolated catalytic domain-containing C-terminal fragment of CheB (residues 147-349) showed that the increased solvent accessibility was less than would have occurred upon detachment of the regulatory domain. Thus, phosphorylation causes subtle changes in solvent accessibility at the interdomain interface of CheB.

Keywords: MALDI-TOF; H/^{2}H exchange; chemotaxis; response regulator; phosphoaspartate

In ''two-component'' signal transduction pathways, stimulus-response coupling is mediated by His-Asp phosphotransfers between histidine kinases and their cognate response regulators.[1] Response regulators have a phosphoaccepting regulatory domain with a conserved fold containing the site of phosphorylation, a single conserved aspartate residue, and an associated effector domain.[2] It is as yet unclear how phosphorylation-dependent conformational changes within the regulatory domains are communicated to associated effector domains leading to modulation of activity within the effector domains. What is clear is that activation must happen rapidly due to the labile nature of the phosphoaspartate.

Structural changes are known to occur upon phosphorylation of regulatory domains of response regulators. The phosphorylated state is characterized by the reorientation of a few conserved side-chains, a Ser/Thr that forms a hydrogen bond with the γ-phosphoryl group and a Phe/Tyr that adopts an inward orientation, occupying a cavity vacated by the Ser/Thr. The propagated conformational change induced by phosphorylation has

Abbreviations used: MALDI-TOF, matrix-assisted laser desorption ionization-time-of-flight; MS, mass spectrometry; TFA, trifluoroacetic acid.

E-mail address of the corresponding author: ekomives@ucsd.edu

0022-2836/01/040967–10 $35.00/0

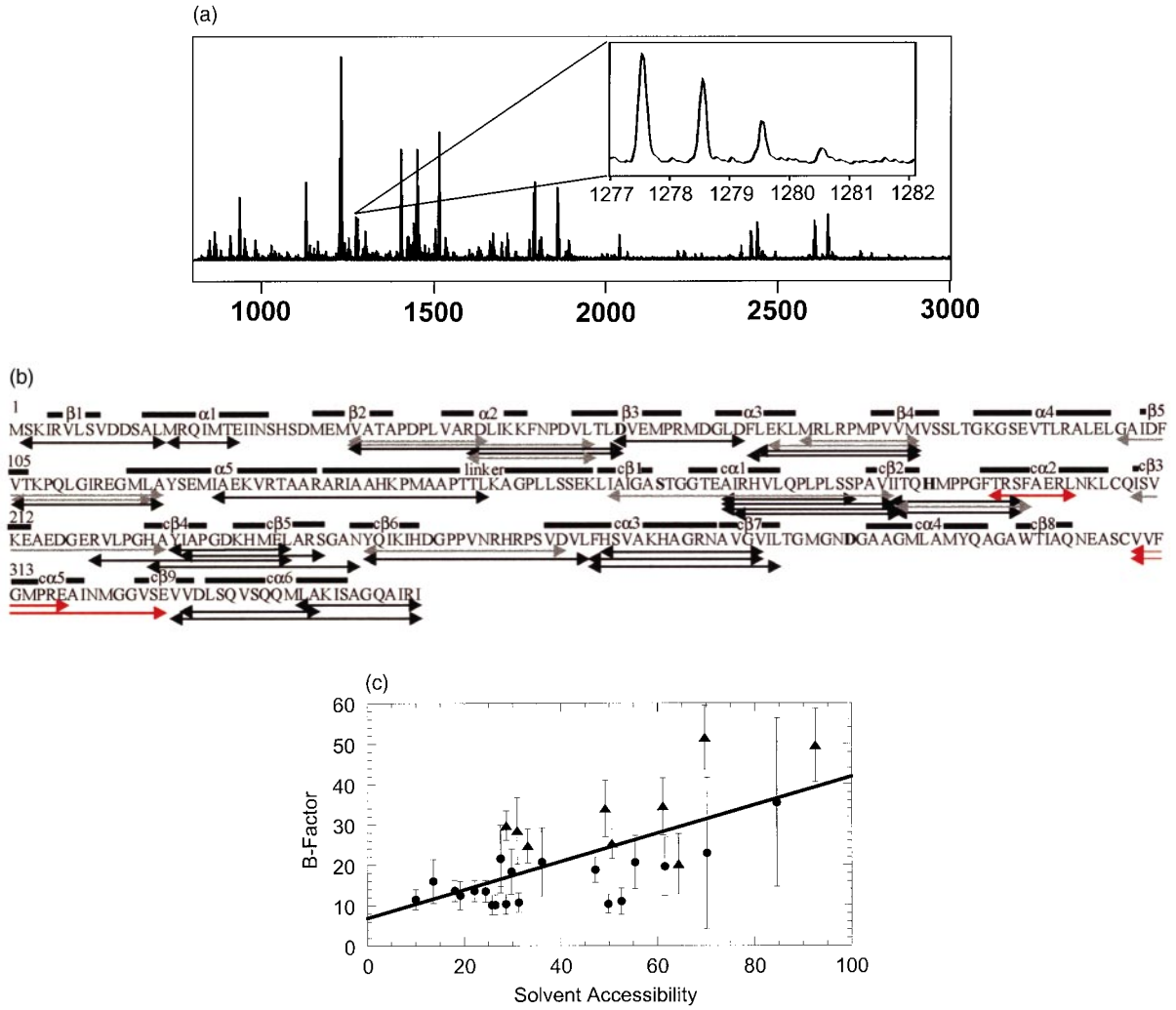

Figure 1. MALDI-TOF mass spectrometric analysis of the peptic digest and overall solvent accessibility of methylesterase CheB. The wild-type and Asp56Asn mutant proteins were expressed and purified as previously described and protein concentrations were determined by absorbance at 280 nm.[11] Before each experiment, the ammonium sulfate concentrates of each protein were dialyzed overnight against 50 mM Tris-HCl, 50 mM NaCl, 1 mM EDTA, and 2.8 mM β-mercaptoethanol (pH 8.0) and aliquoted (1 nmol/tube) into 0.5 ml microcentrifuge tubes, lyophilized, and stored at −80 °C. One tube of protein was resuspended in 130 µl of 0.1 % TFA (pH 2.5) and digested with a 2:1 molar ratio of immobilized pepsin for five minutes. MALDI-TOF mass spectrometry was carried out on a PE Biosystems Voyager DE-STR instrument using a matrix of 5 mg/ml α-cyano-4-hydroxycinnamic acid in a 1:1:1 mixture of acetonitrile, ethanol, and 0.1 % TFA (pH 2.2). (a) MALDI-TOF mass spectrum of the complete peptic digest from CheB without any HPLC separation. The inset is an expansion of the spectrum showing the mass envelope at 1277.56 for the wild-type corresponding to residues 56-66. The different peaks in the envelope are the isotopic peaks. (b) Sequence of CheB showing the peptides that were observed in the mass spectrum of the peptic digest. Peptides were identified by a combination of post-source decay and carboxypeptidase Y sequencing as described previously.[14,15] No differences were observed in the mass spectra of pepsin cleavage products for the Asp56Asn CheB (other than for the peptide containing the mutation), or for phosphorylated CheB compared to wild-type. The phosphoaspartate is labile, and no phosphopeptides were observed in the mass spectra. Pepsin cleavage of CheBc (CheB fragment corresponding to residues 147-349) generated all the same peptides already identified from the C-terminal domain of full-length CheB. Two peptides corresponding to residues 171(2)-186(7) and 338(9)-348(9) had ambiguous termini (Leu/Ile). In the text, we refer to the latter as 339-349. Black lines indicate peptides for which quantifiable data were obtained and gray lines indicate those for which quantifiable data could not be obtained due to overlapping mass envelopes upon deuteration or due to insufficient signal to noise once the envelope broadened due to deuteration. The secondary structural elements are indicated above the sequence. Peptides for which increases in solvent accessibility were seen upon phosphorylation are colored red. (c) The number of deuterons incorporated into each region of CheB within five minutes correlated with the average backbone crystallographic *B* factor for each region (see the legend to Figure 2 for experimental conditions). Fragments of the regulatory domain (▲) generally had higher solvent accessibility than fragments of the catalytic domain (●) and errors are the standard deviation for the average *B* factor (*y*-axis) or for the average solvent accessibility (*x*-axis).

different magnitudes and covers different subsets of the molecular surface in different response regulatory domains.[3–8]

Methylesterase CheB is one of two response regulators in the bacterial chemotaxis system. It catalyzes the deamidation of specific glutamines and demethylation of specific methylglutamate residues introduced into the chemoreceptors by the methyltransferase CheR, thereby contributing to signal adaptation.[9] CheB has an N-terminal regulatory domain joined by a linker to a C-terminal effector domain with methylesterase activity.[10] The C-terminal domain alone (CheBc) possesses tenfold greater methylesterase activity than intact, unphosphorylated CheB indicating an inhibitory role for the regulatory domain. Phosphorylation of CheB at Asp56 results in a tenfold stimulation of methylesterase activity above that seen for CheBc, suggesting that the regulatory domain also contributes positively to enzymatic activity.[11] The structure of unphosphorylated CheB reveals a large interdomain interface with the regulatory domain sterically blocking access of substrate to the methylesterase active site.[12] Enhancement of methylesterase activity upon phosphorylation would therefore be expected to involve a repositioning of the domains to relieve inhibition, and perhaps formation of new contacts that promote catalysis.

Proteolytic sensitivity studies designed to probe phosphorylation-dependent conformational changes showed an increase in proteolytic sensitivity of the linker between the regulatory and catalytic domains, as well as a decrease in proteolytic sensitivity of the loop connecting strand β5 and the α5 helix within the regulatory domain.[13] These results suggested that perhaps more subtle changes were occurring upon transient phosphorylation. A more sensitive probe of changes in domain-domain interactions can be obtained from observation of amide hydrogen/deuterium ($H/^2H$) exchange of the rapidly exchanging amides.[14] These experiments probe changes in protein-protein interfaces by measurement of changes in accessibility of the solvent accessible amides.[15] We therefore set out to characterize the solvent accessibility changes that occur upon phosphorylation of CheB. Comparison of results from phosphorylated and unphosphorylated full length CheB, from the Asp56Asn mutant of CheB that cannot be phosphorylated, and from the catalytic domain fragment of CheB[16] (residues 147-349) reveal subtle changes upon phosphorylation.

Solvent accessibility of the rapidly exchanging amides in CheB

The experiment was set up so as to observe changes in the number of amides that were rapidly exchanging in the native state ensemble of folded protein structures. Equation (1) represents the kinetic parameters of the experiment wherein the ''closed'' structure is the inactive form and the ''open'' structure is the active form of methylesterase CheB:

$$(H)\mathrm{CheB}_{Cl} \overset{\rightarrow}{\leftarrow} \mathrm{CheB}_{Op} \xrightarrow{k_{ex}} (^2H)\mathrm{CheB} \qquad (1)$$

In this experiment, the closed and open states of CheB are in rapid equilibrium, with the closed state being favored in the unphosphorylated protein. Upon phosphorylation, the equilibrium distribution between the open and closed state changes (equation (2)):

$$(H)\mathrm{CheB}_{Cl} \overset{\leftarrow}{\rightarrow} \mathrm{CheB}_{Op} \xrightarrow{k_{ex}} (^2H)\mathrm{CheB} \qquad (2)$$

The rate of amide $H/^2H$ exchange, k_{ex}, cannot be precisely determined because it is the exchange rate of amides in a folded protein. Although the rates of exchange are uninterpretable, the number of deuterons on a particular segment of the protein indicates the solvent accessibility of the rapidly exchanging amides in that segment of the protein. We have previously shown that the solvent accessibility of the rapidly exchanging amides measured in this way is a good indicator of the presence of a protein-protein interface.[15] Thus, the experiment will show whether the protein-protein interface between the regulatory and catalytic domain of CheB differs when the new equilibrium between open and closed states is established upon phosphorylation.

After $H/^2H$ exchange, the reaction was quenched by tenfold dilution into cold 0.1 % (v/v) trifluoroacetic acid to rapidly lower the temperature to 0 °C and the pH to 2.5. Only backbone amides retain deuterium under these conditions. All the rapidly exchanging side-chain protons rapidly exchange to the final percent deuterium upon dilution (5 % for the experiments presented here).[14] The experimental set-up allowed direct comparison of amide deuteration levels for all regions of the protein simultaneously because there was no need for peptide separation steps.

In order to localize the observed solvent accessibility changes to regions of CheB, the protein was cleaved by pepsin under quench conditions. All of the resulting peptide fragments of CheB were then analyzed for deuterium content in a single MALDI-TOF (matrix-assisted laser desorption/ionization time-of-flight) mass spectrum of the mixture of the peptic peptides without any intervening purification steps. Prior to the $H/^2H$ exchange experiment, the 40 peptides resulting from pepsin cleavage of CheB were identified (Figure 1(a) and (b)). Wild-type and Asp56Asn mutant CheB proteins gave exactly the same digest patterns except for the fragment encompassing residues 56-66 (m/z 1277.56) that has a molecular mass difference of 1 mass unit because the asparagine side-chain has a molecular mass 1 mass unit less than the aspartic acid side-chain. In all, the fragments covered 78 % of the entire sequence. Quantitative measurement of the deuterium incorporation was possible for 71 % of the entire protein (Figure 1(b)). Quantifi-

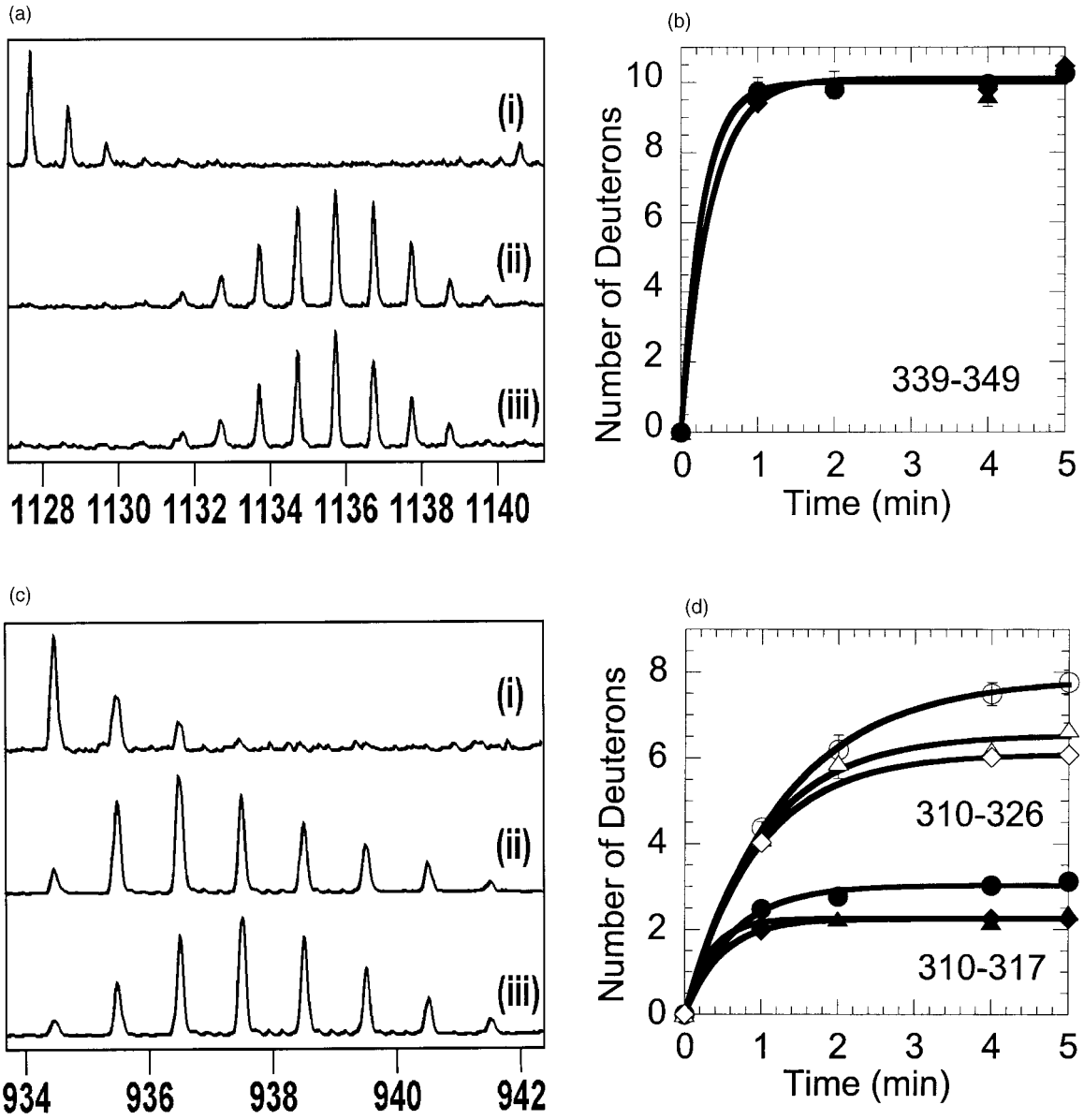

Figure 2 (*legend opposite*)

able data could not be obtained for a few peptides because the mass envelopes overlapped upon deuteration or because of insufficient signal to noise once the envelope broadened due to deuteration. A similar amount of coverage was obtained for both the regulatory and catalytic domains. MALDI-TOF mass spectrometry was chosen as the method of analysis for these amide $H/^2H$ exchange experiments because all of the peptide fragments can be rapidly and easily analyzed in a single spectrum facilitating internal comparisons. The disadvantage is that coverage of the entire protein sequence is usually less than 100 %, a phenomenon that may be due to suppression effects.

Solvent accessibility of each region of CheB was quantitatively measured as the number of deuterons that were rapidly incorporated, which was taken to be the number of deuterons incorporated within five minutes (Table 1). Because the exchange rates are uninterpretable, only changes in the number of deuterons incorporated and not the rates of exchange were considered, although data were obtained for on-exchange times of one to five minutes to assess reproducibility. The numbers of deuterons incorporated were corrected for back exchange, which was assessed by analysis of samples of CheB and mutant CheB that were deuterated for 24 hours. By 24 hours, two segments appeared to have exchanged completely, and these were used to determine the extent of back exchange (22.4 %), and all the data was subsequently corrected by this value. Solvent accessibility was measured as the number of deuterons incorporated after five minutes divided by the

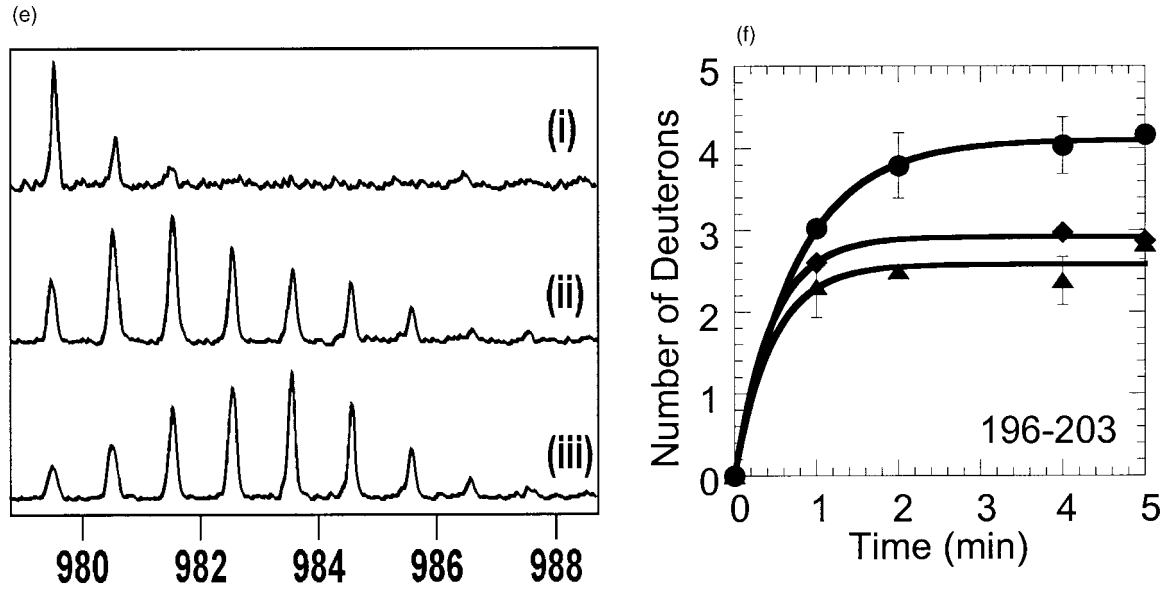

Figure 2. Changes in solvent accessibility upon phosphorylation of full-length CheB. Incorporation of solvent deuterons from buffered ^2H_2O into full-length CheB and the Asp56Asn mutant of CheB was carried out in the presence of phosphoramidate, a reagent that phosphorylates Asp56 of CheB. The lyophilized, buffered proteins were resuspended in 6 μl of ^2H_2O containing 25 mM $MgCl_2$, 10 mM β-mercaptoethanol. After 30 seconds, 6 μl of deuterated phosphorylating solution containing 500 mM phosphoramidate[13] 25 mM $MgCl_2$, 10 mM β-mercaptoethanol, was added. Exchange ($p^2H = 7.4$) at room temperature occurred for 1-5 minutes for determination of solvent accessibility or for 24 hour for determination of the back exchange correction factor. After exchange, the reaction was quenched by dilution into 124 μl of pre-chilled (0 °C) H_2O containing enough 2 % TFA to result in a final solution of approx. 0.1 % TFA (pH 2.5). The quenched protein was digested with a 2:1 molar ratio of immobilized pepsin for five minutes. After centrifugation, the supernatant was frozen in liquid N_2, and stored at −80 °C. The matrix and MALDI target plates were kept at 4 °C prior to use. Frozen samples were rapidly defrosted to 0 °C, mixed 1:1 with matrix, and spotted on the pre-chilled targets. The targets were dried as previously described and only one sample was analyzed within three minutes to minimize back exchange.[14] The average number of deuterons present on each peptide was determined as the difference between the centroid of the isotopic peak cluster for the deuterated sample compared to the undeuterated control as described.[14,22] The curves were fit to a single exponential. (a) Mass spectrum showing the mass envelope of a representative region of CheB that did not change upon phosphorylation. The peak corresponds to mass 1127. 68 (residues 339-349) of (i) CheB without deuteration; (ii) Asp56Asn mutant CheB deuterated for five minutes in the presence of phosphoramidate; and (iii) CheB deuterated for five minutes in the presence of phosphoramidate. (b) Plot of the deuterium incorporation into the same region of CheB (residues 339-349). No differences in deuterium incorporation were observed for the Asp56Asn mutant CheB (▲), wild-type CheB in the presence of phosphoramidate (●), or absence of phosphoramidate (◆). (c) Mass spectra showing the mass envelope of the peak at 934.48 (residues 310-317). Spectra (i) through (iii) are the same as in (a). (d) Plot of deuterium incorporation into the region of CheB from residues 310-317 (filled symbols) and residues 310-326 (open symbols). Incorporation into the Asp56Asn mutant CheB (△) and into CheB in the absence of phosphoramidate (◇) was significantly lower than incorporation into CheB in the presence of phosphoramidate (○) with a difference of 0.7 deuterons for both longer and shorter segments. (e) Mass spectra showing the mass envelope of the peak at 979.53 (residues 196-203). Spectra (i) through (iii) are the same as in (a). (f) Plot of deuterium incorporation into the amide positions of the region of CheB from residues 196-203. Incorporation was observed for the Asp56Asn mutant CheB (▲), wild-type CheB in the presence of phosphoramidate (●), or absence of phosphoramidate (◆). An increase of 1.2 deuterons was observed to be incorporated when CheB was phosphorylated.

theoretical possible, and ranged from 9 % to 89 %. The regulatory domain was more solvent accessible than the catalytic domain, and overall, the solvent accessibility of the rapidly exchanging amides correlated well with crystallographic *B* factors (Figure 1(c)). Although others have reported a lack of correlation between crystallographic *B* factors and protection factors (the ratio of a free amide exchange rate *versus* that for the same amide in a structured protein for a slowly exchanging amide; rate differences of $>10^3$), the amount of deuteration of rapidly exchanging amides within segments of CheB does seem to correlate with the crystallographic *B* factors ($R = 0.68$).[17]

Solvent accessibility changes upon phosphorylation of CheB

To compare the solvent accessibility of the phosphorylated state with the non-phosphorylated state, an excess of phosphorylating agent was added to shift the equilibrium (cf. equation (2)) to

Table 1. Summary of H/^{2}H Exchange Data for CheB

Region of CheB	Expected no. of deuterons[a]	Incorporation of deuterons at 24 hours[b]	Wild-type no. of deuterons[c]	D56N mutant no. of deuterons	Wild-type-P no. of deuterons	Cat domain no. of deuterons	% solvent accessibility[d]
A. *Regulatory domain*							
2-14 (β1-α1; 1402.78)	12.85	7.4 ± 0.1	3.8 ± 0.1	4.1 ± 0.1	4.0	N/A	30
15-21(α1; 908.43)	6.65	5.8 ± 0.1	1.8 ± 0.1	1.7 ± 0.2	1.7	N/A	27
32-55 (β2-β3; 2606.50)	21.1	14.9 ± 0.4	10.3 ± 0.2	10.4 ± 0.2	10.1	N/A	49
42-55 (α2-β3; 1671.99)	13.00	7.7 ± 0.2	4.2 ± 0.1	4.3 ± 0.1	4.2	N/A	32
D56-66 (β3-α3;1277.56)	**9.65**	**7.0 ± 0.1**	**6.5 ± 0.1**		**6.4**	**N/A**	**67**
N56-66 (β3-α3;1276.56)	**9.70**	**6.7 ± 0.4**		**6.6 ± 0.1**		**N/A**	**68**
67-81 (α3-β3; 1860.04)	12.90	12.9 ± 0.1*	7.6 ± 0.2	7.5 ± 0.3	N/A	N/A	59
68-81 (α3-β3; 1712.97)	11.90	11.9 ± 0.1*	5.6 ± 0.1	5.5 ± 0.2	5.3	N/A	47
105-118 (β5-α5; 1512.86)	**12.80**	**11.0 ± 0.2**	**11.4 ± 0.2**	**11.5 ± 0.6**	**11.4**	**N/A**	**89**
123-147 (α5-linker; 2644.51)	**23.55**	**19.7 ± 0.5**	**14.6 ± 0.4**	**14.9 ± 0.2**	**14.7**	**N/A**	**62**
B. *Catalytic domain*							
170-182 (cα1; 1424.73)	10.75	5.5 ± 0.2	3.1 ± 0.1	3.2 ± 0.1	3.0	3.6 ± 0.1	29
170-185 (cα1-cβ2; 1698.02)	12.75	6.4 ± 0.1	3.5 ± 0.2	3.4 ± 0.1	3.6	4.5 ± 0.1	27
170-186 (cα1-cβ2; 1811.10)	13.75	6.0 ± 0.1	3.5 ± 0.1	3.4 ± 0.1	3.5	4.8 ± 0.1	25
171(2)-186(7) (cα1-cβ2; 1740.04)	12.75	5.2 ± 0.1	3.2 ± 0.3	3.1 ± 0.1	3.2	3.6 ± 0.1	25
186-198 (cβ2-cα2; 1484.79)	**10.80**	**6.9 ± 0.1**	**6.4 ± 0.1**	**6.5 ± 0.1**	**6.5**	**4.5 ± 0.1**	**59**
187-198 (cβ2-cα2; 1371.67)	**9.80**	**6.4 ± 0.1**	**5.2 ± 0.1**	**5.1 ± 0.1**	**5.4**	**4.8 ± 0.1**	**55**
196-203 (cα2; 979.52)	**7.85**	**5.9 ± 0.1**	**3.6 ± 0.1**	**2.4 ± 0.2**	**2.5**	**5.0 ± 0.2**	**46**
219-236 (cβ4-cβ5; 2004.02)	15.95	6.0 ± 0.1	2.1 ± 0.1	2.2 ± 0.3	2.2	2.2 ± 0.1	13
224-242 (cβ4-cβ6; 2038.02)	18.10	12.1 ± 0.1	4.8 ± 0.1	4.9 ± 0.1	4.9	5.4 ± 0.2	27
226-236 (cβ4-cβ5; 1273.6219)	9.60	4.8 ± 0.1	2.8 ± 0.1	2.7 ± 0.1	2.8	2.5 ± 0.1	29
227-239 (cβ4-cβ5; 1698.01)	11.85	6.4 ± 0.1	3.5 ± 0.2	3.4 ± 0.1	3.6	4.5 ± 0.1	29
243-263 (cβ2-cα3; 2440.30)	18.45	12.0 ± 0.1	6.4 ± 0.1	6.6 ± 0.2	6.5	6.9 ± 0.1	35
264-277 (cα3-cβ7; 1450.77)	13.95	7.1 ± 0.1	3.0 ± 0.1	3.1 ± 0.1	3.2	3.4 ± 0.3	22
264-280 (cα3-cβ7; 1776.03)	16.95	7.1 ± 0.1	3.1 ± 0.1	3.3 ± 0.1	3.1	3.2 ± 0.1	18
265-277 (cα3-cβ7; 1303.71)	12.95	6.7 ± 0.1	3.0 ± 0.1	3.0 ± 0.1	3.0	3.3 ± 0.2	23
310-317 (cα5-cβ5; 934.49)	**6.50**	**5.2 ± 0.2**	**3.1 ± 0.1**	**2.4 ± 0.1**	**2.2**	**4.5 ± 0.1**	**48**
310-326 (cα5-cβ9; 1792.89)	**15.70**	**14.6 ± 0.2**	**7.8 ± 0.3**	**6.7 ± 0.2**	**6.4**	**12.4 ± 0.1**	**51**
327-349(cβ9-Cterm; 2455.41)	23.20	20.9 ± 0.5	15.7 ± 0.2	15.8 ± 0.1	15.7	16.1 ± 0.1	68
328-339 (cα6; 1318.67)	11.65	2.3 ± 0.1	1.1 ± 0.1	1.1 ± 0.1	1.1	1.4 ± 0.1	9
338(9)-348(9) (cα6-Cterm; 1127.68)	**10.75**	**8.7 ± 0.4**	**8.8 ± 0.2**	**9.0 ± 0.2**	**9.0**	**8.8 ± 0.2**	**82**

[a] Equal to the number of amides (not including the N-terminal) plus 5% of the total number of other exchangeable sites due to sample dilution and drying.[14]

[b] All numbers of deuterons were corrected for the 22.4% back exchange calculated from the two segments (*) that completely exchanged after 24 hours. Errors are standard deviations of the mean (three independent determinations).

[c] All data are the number of deuterons incorporated by five minutes. Errors are standard deviation of the mean (three independent determinations). Wild-type-P was only done once.

[d] Equal to the ratio of the number of deuterons incorporated by five minutes compared to the expected number of deuterons.

greater than 70% phosphorylated state over the time course of the experiment[13] despite the short (approximately two seconds) lifetime of the phosphorylated state.[18] Previous experiments have shown that phosphorylation of other sites on the protein is minimal under these conditions.[19] Upon dilution into the quench solution, the aspartyl phosphate is rapidly lost, and no phosphopeptides were observed in the mass spectrum. The solvent accessibility of the phosphorylated form of CheB was compared to unphosphorylated CheB and to an unphosphorylatable mutant of CheB (Asp56Asn) in the presence of phosphorylating reagent. The region of the CheB regulatory domain encompassing the phosphorylation site (residues 56-66, peptide m/z 1277.65 for wild-type CheB and 1276.55 for the Asp56Asn mutant) showed higher deuterium incorporation in the mutant than in the wild-type protein, but no differences were observed in this region upon phosphorylation (Table 1). It is likely that the increased deuterium incorporation in the mutant is due to its inability to bind Mg^{2+} as in the analogous mutant of CheY.[20] This was the only difference in solvent accessibility we observed in the regulatory domain, and it was clearly due to the Asp56Asn mutation, not to phosphorylation.

Other regions of the regulatory domain that might have been expected to show changes upon phosphorylation did not. These include the region encompassing residues 105-118 (peptide m/z 1512.86), which begins one residue after Phe 104, the conserved aromatic residue that is known to change conformation in other response regulators upon phosphorylation. Deuterium incorporation levels showed that this region was highly solvent accessible, but no differences in solvent accessibility were observed between phosphorylated and unphosphorylated CheB (Table 1). Overlapping peptides encompassing residues 67 and 68-81 (m/z 1860.04 and m/z 1712.97) covered strand β4 and also did not change solvent accessibility upon phosphorylation. These regions were not highly solvent accessible, and should have increased in

solvent accessibility if a reorientation of helix α4, such as was reported for phosphorylated NtrC, had occurred. The linker region residues contained within the fragment 123-147 (peptide m/z 2644.51) were also highly solvent accessible and did not become more solvent accessible upon phosphorylation (Table 1) even though it becomes more proteolytically sensitive.[13] The lack of changes in solvent accessibility of the regulatory domain suggests it probably remains in contact with the catalytic domain after phosphorylation.

Most of the catalytic domain of CheB (17 peptides covering 65% of the sequence) showed no significant changes in solvent accessibility upon phosphorylation. Mass spectra and kinetic plots of deuterium incorporation for one such region, residues 338-349 (peptide m/z 1127.68), are shown in Figure 2(a) and (b). Two regions of the catalytic domain of CheB did show significant changes in solvent accessibility upon phosphorylation. The first, represented by two overlapping proteolytic fragments, residues 310-317 (peptide m/z 934.49) and 310-326 (peptide m/z 1792.88) incorporated a significant fraction of additional deuterons in the phosphorylated state (Figure 2(c) and (d)). Since the same fraction of additional deuterons was incorporated into both the longer and shorter peptides, the region of increasing solvent accessibility must lie within residues 310-317. This region connects cβ8 to cα5 and contains Val310 and Val311, which appear to contact the regulatory domain in the crystal structure of CheB. A second region of CheB represented by a single peptide fragment encompassing residues 196-203 (peptide m/z 979.52) also increased solvent accessibility upon phosphorylation (Figure 2(e) and (f)). Again, the region of increased solvent accessibility could be narrowed down because two other fragments encompassing residues 187-198 (m/z 1371.67) and 186-198 (m/z 1484.79) did not show changes in solvent accessibility upon phosphorylation. Thus, the region of increased solvent exposure must lie within residues 199-203. This region corresponds to cα2 in the catalytic domain, and contains the important interdomain contact, Arg202. In sum, only two regions corresponding to the edges of the catalytic domain that contact the regulatory domain increased solvent accessibility upon phosphorylation (Figure 3).

Solvent accessibility of the catalytic domain of CheB in the presence and absence of the regulatory domain

Relatively few changes were observed in the interface between the regulatory and catalytic domains upon phosphorylation. Either the regulatory domain remained largely in contact with the catalytic domain, or the interface of the catalytic and regulatory domain was not really protected

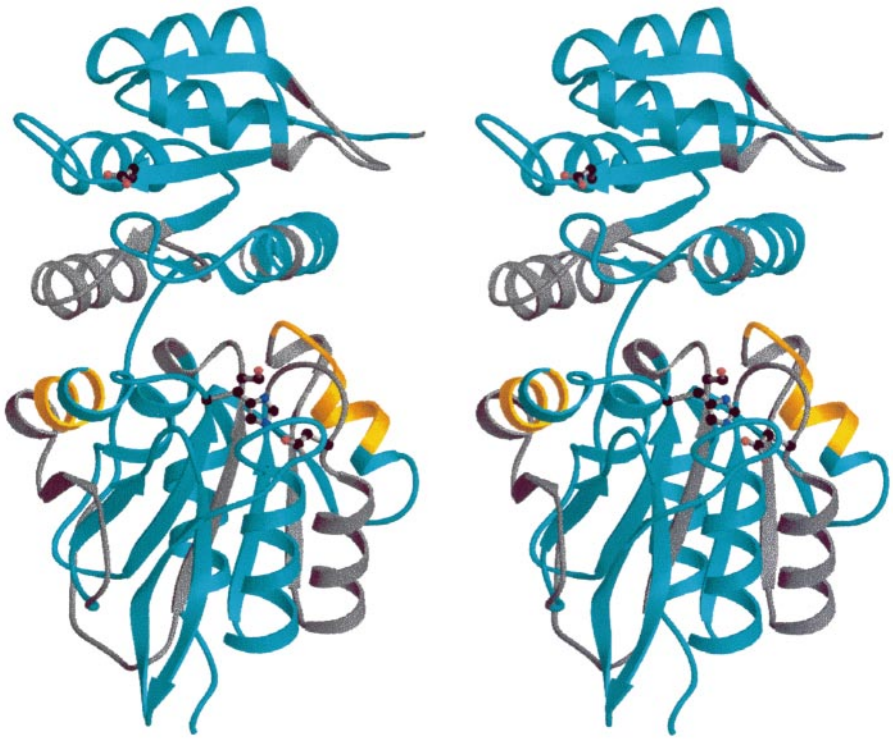

Figure 3. Changes in solvent accessibility of CheB upon phosphorylation. Stereoview of the structure of CheB (PDB accession code 1a2o). The phosphorylation site, Asp56, and active site residues are in ball-and-stick representation, the regions not quantitatively covered by the peptic fragments are gray, the regions quantitatively covered by the peptic fragments that show no changes in deuterium incorporation upon phosphorylation are cyan, the regions that showed increased deuterium incorporation upon phosphorylation are gold.

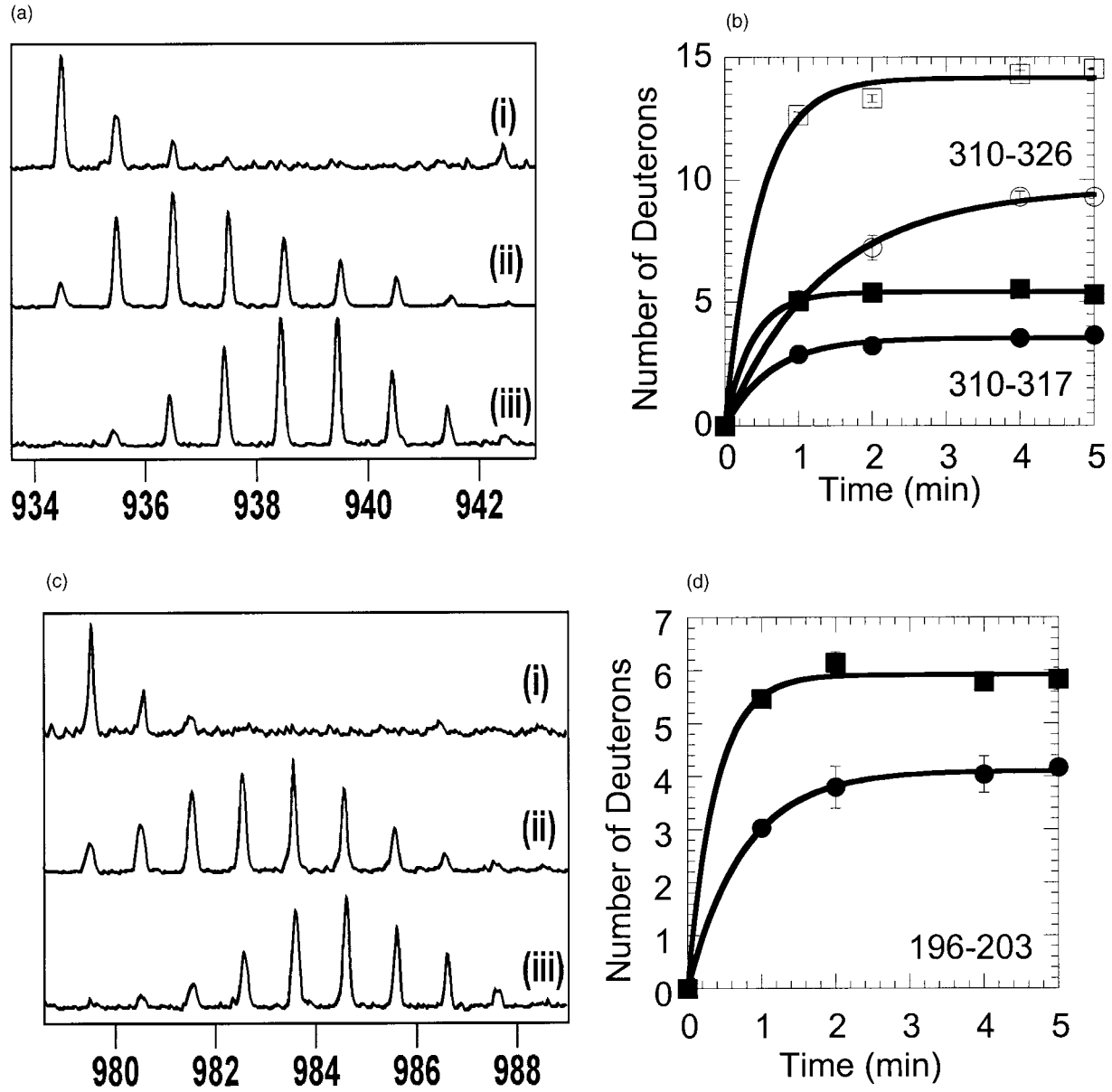

Figure 4 (*legend opposite*)

from solvent. In order to distinguish these possibilities, experiments were performed to compare deuterium incorporation into the catalytic domain fragment, CheBc (residues 147-349) with full-length CheB. The results (Table 1) showed that in the absence of the regulatory domain, certain regions of the catalytic domain were more solvent accessible than they were in the presence of the regulatory domain. Figure 4(a) and (b) shows that the overlapping regions spanning residues 310-317 (peptide m/z 934.49), and 310-326 (peptide m/z 1792.88) incorporated much more deuterium when the regulatory domain was not present than in phosphorylated CheB. On the other side of the catalytic domain, residues 196-203 (peptide m/z 979.52) also incorporated much more deuterium when the regulatory domain was not present (Figure 4(c) and (d)). Residues abutting the linker including 170-185 and 328-339 also incorporated more deuterium in CheBc than in full-length CheB (Table 1). One region spanning residues 186-198 (peptides m/z 1371.67 and m/z 1484.79) showed lower solvent accessibility in CheBc compared to full-length CheB (Table 1). This region is adjacent to the segment 196-203 that increases solvent accessibility, so the results were not completely conclusive. Nevertheless, it is interesting that the 186-198 segment contains the catalytic histidine residue, and it is possible that dynamic conformational differences in this region may partly explain why

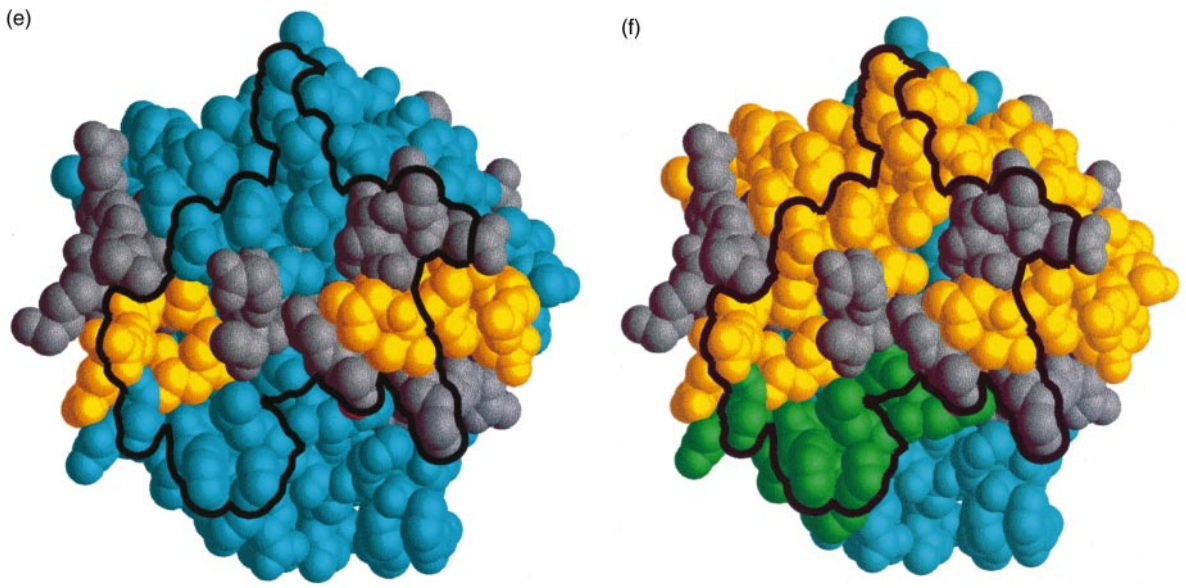

Figure 4. Solvent accessibility of regions of the C-terminal fragment of CheB (CheBc) compared to the same regions of full-length CheB. The exchange reactions were carried out as described in the legend of Figure 2. (a) Mass spectra showing the isotopic envelope for the peptide corresponding to residues 310-317 (i) in the full-length protein before deuteration; (ii) CheB deuterated for five minutes in the presence of phosphoramidate; and (iii) CheBc deuterated for five minutes. (b) Plot of deuterium incorporation into the amide positions of the region of CheB from residues 310-317 (filled symbols) and residues 310-326 (open symbols). Deuterium incorporation into amides of CheBc was much higher (□) than incorporation into this region of full length CheB (○). (c) Mass spectra showing the isotopic envelope for the peptide corresponding to residues 196-203 (i) through (iii) are the same as in (a). (d) Plot of deuterium incorporation into residues 196-203. Plot symbols are the same as in (b). (e) Space filling model of the catalytic domain of CheB showing differences in deuterium incorporation upon phosphorylation. The view is rotated approximately 120° about the *x*-axis relative to that shown in Figure 3 and a black outline shows where the regulatory domain would footprint onto the catalytic domain as determined by solvent accessible surface area calculations of the structure of intact CheB. (f) Space-filling model of the catalytic domain of CheB rotated as in (e) Differences in deuterium incorporation for CheBc compared to full-length CheB showing those regions that were more solvent accessible when the regulatory domain was absent.

phosphorylated CheB is more active than CheBc. Thus, several regions of the catalytic domain that contact the regulatory domain in full-length CheB were more solvent accessible in its absence while one region appeared to be less solvent accessible.

Conclusions

The lack of change in solvent accessibility of the regulatory domain shows that it neither unravels nor tips back to ''open up'' the domain interface upon phosphorylation. The activation mechanism appears to be much more subtle.

Addition of phosphorylating reagent shifts the equilibrium to the open, active form of CheB, and the ''open'' form has increased solvent accessibility of cα2 (residues 199-203) and cα5 (residues 310-317), the edges of the catalytic domain that interface with the regulatory domain (Figure 4(e)). These regions both contain residues that are seen to directly interact with the regulatory domain in the crystal structure of CheB.[12] GRASP[21] calculations of the solvent accessible surface area of the crystallographic model of CheB showed that when the regulatory domain is removed, the increase in solvent accessible surface area of the 199-203 region is entirely accounted for by exposure of Arg202. Similarly, removal of the regulatory domain results in an increase in solvent accessible surface area of the 310-317 region that is entirely accounted for by exposure of Val310 and Val311.

The shift in equilibrium upon phosphorylation opens access to the active site, but does not completely ''pop the lid'' of the regulatory domain. Deuterium incorporation into both the cα2 (residues 199-203) and cα5 (residues 310-317) regions is increased upon phosphorylation but is even higher when the regulatory domain is removed all together (Figure 4(a)-(d)). Furthermore, other regions of the catalytic domain that are buried under the linker are highly solvent accessible in CheBc, but show no increase in solvent accessibility upon phosphorylation (Figure 4(e)-(f)). Thus, only the edges of the catalytic domain become more solvent accessible, but the linker and regulatory domain do not detach. We earlier hypothesized that if Phe104 underwent the same conformational change to an inward conformation as is seen in other response regulators upon phosphorylation, the domain interface would be disrupted.[12]

Instead, although it is very likely that Phe104 does undergo a conformational change analogous to other response regulators, we see only subtle changes at the interface, which is not completely disrupted upon phosphorylation. These results are consistent with the idea that the regulatory and catalytic domains remain in contact and work together to achieve maximal catalytic activity in phospho-CheB.

References

1. Hoch, J. A. & Silhavy, T. J. (1995). *Two-component Signal Transduction*, American Society of Microbiology Press, Washington DC.
2. Volz, K. (1993). Structural conservation in the CheY superfamily. *Biochemistry,* **32**, 11741-11753.
3. Halkides, C. J., McEvoy, M. M., Casper, E., Matsumura, P., Volz, K. & Dahlquist, F. W. (2000). The 1.9 Å resolution crystal structure of phospho-CheY , an analog of the active form of the response regulator, CheY. *Biochemistry,* **39**, 5280-5286.
4. Cho, H. S., Lee, S.-Y., Dalai, Y., Pan, X., Parkinson, J. S., Kustu, S., Wemmer, D. E. & Pelton, J. G. (2000). NMR structure of activated CheY. *J. Mol. Biol.* **297**, 543-551.
5. Feher, V. A. & Cavanaugh, J. (1999). Millisecond-timescale motions contribute to the function of the bacterial response regulator protein Spo0F. *Nature,* **400**, 289-293.
6. Lewis, R. J., Brannigan, J. A., Muchova, K., Barak, I. & Wilkinson, A. J. (1999). Phosphorylated aspartate in the structure of a response regulator protein. *J. Mol. Biol.* **294**, 9-15.
7. Birck, C., Mourey, L., Gouet, P., Fabry, B., Schumacher, J., Rousseau, P., Kahn, D. & Samama, J.-P. (1999). Conformational changes induced by phosphorylation of the FixJ receiver domain. *Structure,* **7**, 1505-1515.
8. Kern, D., Volkman, B. F., Luginbuhl, P., Nohalle, M. J., Kustu, S. & Wemmer, D. (1999). Structure of a transiently phosphorylated switch in bacterial signal transduction. *Nature,* **402**, 894-898.
9. Falke, J. J., Bass, R. B., Butler, S. L., Chervitz, S. A. & Danielson, M. A. (1997). The two-component signaling pathway of bacterial chemotaxis: a molecular view of signal transduction by receptors, kinases, and adaptation enzymes. *Annu. Rev. Cell. Dev. Biol.* **13**, 457-512.
10. Simms, S. A., Keane, M. G. & Stock, J. (1985). Multiple forms of the CheB methylesterase in bacterial chemosensing. *J. Biol. Chem.* **260**, 10161-10168.
11. Anand, G. S., Goudreau, P. N. & Stock, A. M. (1998). Activation of methylesterase CheB: evidence of a dual role for the regulatory domain. *Biochemistry,* **37**, 14038-14047.
12. Djordjevic, S., Goudreau, P. N., Xu, Q., Stock, A. M. & West, A. H. (1998). Structural basis for methylesterase CheB regulation by a phosphorylation-activated domain. *Proc. Natl Acad. Sci. USA,* **95**, 1381-1386.
13. Anand, G. S., Goudreau, P. N., Lewis, J. K. & Stock, A. M. (2000). Evidence for phosphorylation-dependent conformational changes in methylesterase CheB. *Protein Sci.* **9**, 898-906.
14. Mandell, J. M., Falick, A. M. & Komives, E. A. (1998a). Measurement of amide hydrogen exchange by MALDI-TOF mass spectrometry. *Anal. Chem.* **70**, 3987-3995.
15. Mandell, J. M., Falick, A. M. & Komives, E. A. (1998b). Identification of protein-protein interfaces by decreased amide proton solvent accessibility. *Proc. Natl Acad. Sci. USA,* **95**, 14705-14710.
16. West, A. H., Martinez-Hackert, E. & Stock, A. M. (1995). Crystal structure of the catalytic domain of the chemotaxis receptor methylesterase, CheB. *J. Mol. Biol.* **250**, 276-290.
17. Milne, J. S., Mayne, L., Roder, H., Wand, A. J. & Englander, S. W. (1998). Determinants of protein hydrogen exchange studied in equine cytochrome *c*. *Protein Sci.* **7**, 739-745.
18. Stewart, R. C. (1993). Activating and inhibitory mutations in the regulatory domain of CheB, the methylesterase in bacterial chemotaxis. *J. Biol. Chem.* **268**, 1921-1930.
19. Buckler, D. R. & Stock, A. M. (2000). Synthesis of ^{32}P-phosphoramidate for use as a low molecular weight phosphodonor reagent. *Anal. Biochem.* **283**, 222-227.
20. Lukat, G. S., Stock, A. M. & Stock, J. B. (1990). Divalent metal ion binding to the CheY protein and its significance to phosphotransfer in bacterial chemotaxis. *Biochemistry,* **29**, 5436-5442.
21. Nicholls, A., Sharp, K. A. & Honig, B. (1991). Protein folding and association: insights from the interfacial and thermodynamic properties of hydrocarbons. *Proteins: Struct. Funct. Genet.* **11**, 281-296.
22. Zhang, Z. & Smith, D. L. (1993). Determination of amide hydrogen exchange by mass spectrometry: a new tool for protein structure elucidation. *Protein Sci.* **2**, 522-531.

Edited by P. E. Wright

(Received 21 November 2000; received in revised form 22 January 2001; accepted 22 January 2001)